

Global structure and formation of polar-ring galaxies

V. Reshetnikov^{1,2}, N. Sotnikova¹

¹ Astronomical Institute of St.Petersburg State University, 198904 St.Petersburg, Russia

² DEMIRM, Observatoire de Paris, 61 Av. de l'Observatoire, F-75014 Paris, France

Received 1996; accepted

Abstract. We present an analysis of structural features of all known galaxies with optical polar rings. We find a clear dichotomy for objects of this peculiar class. Bulge-dominated S0 galaxies possess only short narrow rings, while disk-dominated objects always have wide extended polar rings. We try by gas dynamical simulations to explain such a segregation by dependence of the ring-forming process on different galaxy potentials. It is found that the total mass captured into the ring during an encounter of a host-ring system with a gas-rich spiral galaxy of comparable mass exceeds $10^9 M_\odot$ (or about 10% of all gas in the donor galaxy), which is of the order of that found by observation. The process of gas to gather into a steady-state ring takes approximately $(7 - 9) \times 10^8$ years. This time is somewhat shorter for rings forming around bulge-dominated galaxies. We also present observational arguments for S0 galaxies with extended rings to be similar to late-type spirals by their photometric properties, while numerical modelling of the extended ring formation suggests that these galaxies must possess massive dark halos as well. In this case, the sizes of the modelled rings turn out large enough (up to 30 kpc in diameter), and the time scale for ring formation is prolonged up to several Gyrs.

Key words: galaxies: general, interactions, photometry, kinematics and dynamics, peculiar, structure - dark matter

1. Introduction

Recent observations (and especially with HST) demonstrate that mutual interactions and mergers between galaxies at early stages of evolution of the Universe were probably among the main processes leading to the observed properties of galaxies (e.g., Keel 1996). Even at the present epoch, at least 5-10% of galaxies are members of interacting systems. Many other galaxies keep signs

in their structure of past interactions and mergings (for example, elliptical and S0 galaxies with inclined gaseous disks, galaxies with faint shells and ripples, galaxies with kinematically decoupled nuclei, etc.).

Polar-ring galaxies (PRGs), consisting of large-scale rings of stars, gas and dust orbiting around major axes of early-type galaxies, may be considered as extreme samples of possible interaction relics. Indeed, in the case of PRGs, the remnants of merged galaxies are not mixed in one smooth object but stay separately in a quasi-steady state for a long time. PRGs are very rare objects. For example, the Polar Ring Catalogue by Whitmore et al. (1990) (PRC) lists only 6 classic kinematically-confirmed polar-ring galaxies.

The unique geometry of PRGs attracts the attention of astronomers trying to test the 3D shape of galactic potentials and to study the stability of inclined rings and disks (see recent review articles by Tohline 1990, Sackett 1991, Sparke 1991, Combes 1994, Cox & Sparke 1996). Such an important question as the origin of these peculiar objects it is still not adequately investigated. It is usually suggested that collapse of a single protogalactic cloud cannot create an object with two nearly-orthogonal large-scale systems (but see Curir & Diaferio 1994), and so some secondary event must occur in the history of PRGs.

Summarizing possible scenarios of polar-ring formation, one can enumerate the following: the accretion of matter from a nearby system or the capture and merging of a gas-rich companion; the delayed inflow of a primordial intergalactic cloud; the accretion of matter from the outskirts of the host galaxy itself; the polar-ring formation from the return of the tidal material during the merging of two gas-rich spirals (Toomre 1977, Shane 1980, Schweizer et al. 1983, Sackett 1991, Sparke 1991, Hibbard & Mihos 1995).

Probably, all the above mechanisms can create ring-like structures around early-type galaxies. To our mind, the most straightforward scenario is the first one. Recent observations of several binary interacting systems clearly demonstrate such rings in the making (for instance, NGC

7464/65 - Li & Seaquist 1994, NGC 3808A,B and NGC 6285/86 - Reshetnikov et al. 1996).

Another unclear question is the nature of central objects in PRGs and a possible correlation of host galaxy properties with characteristics of a surrounding polar ring.

In this paper, we present SPH simulations of polar ring formation around target galaxies of different structures due to gas accretion during the encounter with a comparable-mass spiral galaxy. In our simulations, we try to answer the following main questions: Does this mechanism work? What determines the size of the resulting ring, and what is its spatial structure? On what timescale does the ring form? What is the mass fraction of the gas captured into a ring?

The paper is organized as follows: in Section 2, we examine observational properties of all known kinematically confirmed PRGs and formulate some observational constraints on numerical simulations; in Section 3, we discuss previous attempts to model the PRGs formation, describe our modelling technique and results of simulations; and finally we give our conclusions in Section 4.

Throughout the paper, all distance-dependent quantities are calculated using $H_0 = 75$ km/s/Mpc.

2. General characteristics of polar-ring galaxies

As a definition of a polar-ring galaxy, we will use the definition of Category A objects in the PRC: spectroscopic evidence must exist for two nearly-perpendicular kinematical subsystems; centers of the two components must be aligned, and both subsystems must have similar systemic velocities; the ring must be comparable in size to the host galaxy, must be luminous and nearly planar. This definition allows to separate dust-lane ellipticals, galaxies with inclined HI rings etc. from PRGs. Using this rigorous definition, one can now consider only three additional galaxies to 6 the classic PRGs listed in the PRC: AM 2020-504 (Whitmore & Schweizer 1987, Arnaboldi et al. 1993), IC 1689 (Reshetnikov et al. 1995, Hagen-Thorn & Reshetnikov 1997) and NGC 5122 (Cox et al. 1995). (We do not consider ESO 603-G21 here due to the puzzling kinematics of the central galaxy (Arnaboldi et al. 1995).)

An examination of the optical images of PRGs (e.g. in the PRC) allows one to divide them into two groups (Whitmore 1991): galaxies with extended disk-like rings with the central region cut out and galaxies with relatively narrow rings, not extended in radius. This division is quite distinct since the first group of galaxies - A0136-0801 (A-1), UGC 7576 (A-4), NGC 4650A (A-5), UGC 9796 (A-6), and NGC 5122 (B-16) - possess optical rings extended out to 2-3 diameters of the central galaxies, while the second group - ESO 415-G26 (A-2), NGC 2685 (A-3), IC 1689 (B-3), and AM 2020-504 (B-19) - demonstrate optical rings with size not exceeding the diameter of the host galaxy.

In Table 1, we generalize the main observational characteristics of the two groups of PRGs. (Note that, due to

the absence of optical data about NGC 5122, we did not consider this galaxy in the table.) In the case of incomplete data or large scatter of characteristics, we give in the table only limits or indicate the range of parameter changes. Absolute luminosities and colors in the table are corrected for Galactic absorption.

We discuss Table 1 in detail.

2.1. Central galaxies

The problem of the bulge-to-disk ratio determination for the PRGs is not quite simple. Reshetnikov et al. (1994) have noticed that bulge effective parameters (μ_e and R_e) of PRGs with wide extended rings (our first group) lie in the plane of effective parameters below the mean relationship for normal galaxies (this means that at the same value of μ_e , bulges of PRGs have smaller radii in comparison with bulges of normal galaxies) - see Figure 7 in the cited paper. But bulge characteristics of the second group of galaxies are located exactly along the standard relationship. Such a dichotomy suggests two explanations: the unusual compactness of the first group of PRG bulges or the underestimation of their sizes and luminosities due to the projection of gas and dust rich extended rings on central regions of the galaxies (Reshetnikov et al. 1994).

A comparison of photometric cuts of the galaxies in different color bands allows one to solve this problem. In Figure 1, we present surface brightness distributions for four PRGs with extended rings along the major axes of their central galaxies. We compare two profiles for each galaxy: one in the B passband and other in the red filter (R , i , or K). As one can see from figure, absorption in the rings barely changes the shape of the profiles. Therefore, PRGs with wide extended rings in fact possess unusually compact and faint bulges in comparison with normal early-type galaxies. As is evident from Figure 1, the exponential disk dominates in the photometric structure of all these galaxies. The ratio of the total bulge luminosity to the luminosity of the exponential disk in the first group of PRGs is about 0.1 (we denoted this as $\ll 1$ in Table 1).

The photometric structure of PRGs with short rings (the second group of galaxies) looks usual for early-type galaxies. As was mentioned earlier, their characteristics in the plane of effective parameters follow the mean relation for normal galaxies. According to original papers, bulge-to-disk ratios in the B band for these galaxies are: ESO 415-G26 - 0.52 (Whitmore et al. 1987), NGC 2685 - 0.9 (Makarov et al. 1989), IC 1689 - 1.9 (Reshetnikov et al. 1995). AM 2020-504 is an elliptical galaxy (Arnaboldi et al. 1993). Therefore, the second group PRGs are normal bulge-dominated galaxies by their photometric structure (conditionally, ≈ 1 in the table).

Table 1. General characteristics of PRGs

| Parameter | Extended rings | Short rings |
|-------------------------------------|---|--------------------------------|
| <i>Central galaxy:</i> | | |
| Bulge-to-disk ratio | $\ll 1$ | ≈ 1 |
| Absolute luminosity in the B band | $-18.6 \pm 0.5(\sigma)$ | $-19.2 \pm 0.3(\sigma)$ |
| $B - V$ | $+0.84 \pm 0.05$ | $+0.91 \pm 0.03$ |
| Colour gradient | Yes | Yes |
| σ (km/s) | 80 ± 20 | $100 \div 270$ |
| V_{\max}/σ | 1.7 ± 0.3 | $0.45 \div 1.4$ |
| Decoupled nuclei | ? | Yes |
| <i>Ring:</i> | | |
| Diameter | $\approx (2 - 3)D_{25}$ 26 ± 6 kpc | $\leq D_{25}$ 9 ± 4 kpc |
| Absolute luminosity in the B band | -17.5 ± 0.6 | ≥ -15.4 |
| $B - V$ | -0.1 to $+0.7$ | $+0.2$ to $+0.64$ |
| Colour gradient | Yes | ? |
| HI mass ($10^9 M_{\odot}$) | 6 ± 2 | ≤ 9 |
| Ring inclination | $7^{\circ} \div 26^{\circ}$ | $1^{\circ} \div 16^{\circ}$ |

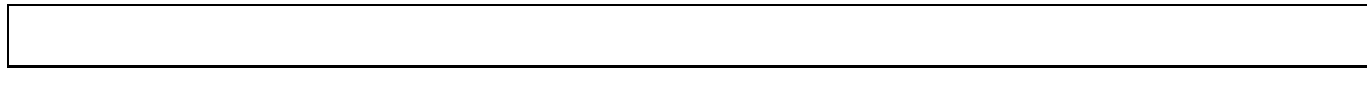


Fig. 1. Photometric profiles of PRGs with extended rings along major axes of the central galaxies. The data for A0136-0801 are from Schweizer et al. (1983) and PRC; NGC 4650A – Whitmore et al. (1987) and Combes & Arnaboldi (1996); UGC 7576 and UGC 9796 – Reshetnikov et al. (1994). The dashed lines represent exponential fits of the observed distributions.

2.2. Polar rings

Rings sizes in the two groups of galaxies are different, as well as their absolute luminosities (D_{25} in Table 1 denotes a diameter of the central galaxy measured at the surface brightness level $\mu_B = 25$). Both groups of rings show a large scatter of optical colors although, as it was shown by Reshetnikov et al. (1995), there is a general trend with a blue surface brightness; bluer rings have, on average, higher surface brightnesses. Extended rings also show large-scale color gradients, that is, they become bluer at larger radii (see, for instance, Figures 4,6 in Reshetnikov et al. 1994 and Arnaboldi et al. 1995). Both group of rings contain a large amount of neutral hydrogen (we assume in Table 1 that all detected HI belongs to the rings), with larger scatter of HI mass in PRGs with narrow rings (Schechter et al. 1984, van Gorkom et al. 1987, Richter et al. 1994). The last line of Table 1 shows the range of ring inclinations (angular distance between the ring and the perpendicular to the central galaxy plane) according to Whitmore (1991). Both groups of PRGs demonstrate rings to be very close to perpendicular, with a somewhat larger deviation for extended rings. It should also be noted that global characteristics of extended rings resemble the disks of spiral galaxies (this was previously pointed out

by Reshetnikov et al. 1994 and Reshetnikov & Combes 1994a,b). We will discuss this analogy in Section 4.

Summarizing the above analysis, one can conclude that *there is a correlation between general properties of optical polar rings and characteristics of host galaxies*. Extended, disk-like rings exist preferably around galaxies which have global photometric structure (and probably mass distribution) similar to late-type spiral galaxies. Host galaxies of PRGs with extended rings demonstrate a remarkable similarity – their characteristics fall in a relatively narrow range (see Table 1). From the other side, bulge-dominated galaxies have tighter and narrow rings. Host galaxies and rings of PRGs with non-extended rings demonstrate significantly larger scatter of intrinsic properties.

Although the statistics of PRGs are not great (8 - 9 objects only), the mentioned tendency is quite distinct – there are no bulge-dominated galaxies with extended luminous polar rings. It is significant since the known PRGs were selected on the base of optical morphology only, without any attention to the structure of the central galaxies. One can note also that the PRG dichotomy is quite analogous to a recently-found difference of ionized gas distribution in elliptical and S0 galaxies. According to Macchetto et al. (1996), more than half of elliptical galaxies with detected ionized gas have their gas concentrated in small (≤ 4 kpc) nuclear disks, while most

S0 galaxies demonstrate more extended (up to 18 kpc) distribution of the gas.

A similar tendency was mentioned for the first time by Whitmore (1991), who found that only rapidly-rotating S0 disks have extended luminous polar rings, while dust-lane ellipticals rarely show an extended luminous component. He suggested that a more flattened potential of the S0 galaxy is able to stabilize the ring at greater radii than in an elliptical galaxy. In the next Section, we will demonstrate that the observed dichotomy could be caused by another reason.

3. Numerical simulations

There are only a few investigations that illustrate several proposed scenarios of polar ring formation. This lack of theoretical study devoted to the question of ring origin is connected with the necessity of the usage of complicated 3D gas dynamics models, since polar rings contain a high amount of neutral gas (up to a few $10^9 M_{\odot}$), as seen from Table 1. One of the most fit tools to construct such models is a smoothed particle hydrodynamics algorithm – SPH, – originally proposed by Lucy (1977) and Gingold & Monaghan (1977) and considerably developed in the late eighties (e.g., Hernquist & Katz 1989). It is fully three-dimensional, flexible regarding the geometry of the gas distribution and consequently well-suited to modelling both the donor and recipient galaxies and the empty extended space between them. Applied to a range of polar-ring investigation problems, this method has already lead to many important results.

The main result of the ring stability investigations is that the time for gas in an axisymmetric or triaxial potential to settle into a steady state is small compared to the age of the Universe (see Christodoulou et al. 1992 and references therein). So there is sufficient time for accreted gas to form polar rings. However, these studies did not take into account time-dependent effects and realistic initial conditions. Some efforts to include these effects have been made by Rix & Katz (1991) and Weil & Hernquist (1993).

Rix & Katz (1991) have treated the polar-ring formation process as a gradual smearing of a small gaseous blob captured by a galaxy of spherically-symmetric structure on a distant circular orbit. Naturally, the diameter of the forming ring (up to 80 kpc) was quite completely dictated by the initial position of a gaseous satellite (the orbit radius). The approach of Weil & Hernquist (1993) was more self-consistent. They have considered a parabolic encounter of a low-mass gas-rich companion with a more massive galaxy and consequent merging of the former. The gaseous component of the satellite was settling into the ring after the total disruption of the satellite in the vicinity of the target galaxy. The forming ring turned out rather small (about 6-7 kpc in diameter) and its size was de-

termined in the end by a hand-introduced description of details of the companion disruption.

The ability of the accreting material to dissipate energy is the crucial factor for ring formation. Test (noninteracting) particles (which imitate molecular clouds from intergalactic space or clouds belonging to a companion galaxy) lose energy due to ram-pressure in an extended halo of a spiral galaxy and form a gaseous ring rotating around the disk of the spiral (Sofue & Wakamatsu 1993, Sofue 1994).

3.1. Modelling of polar-ring characteristics during the ring-forming process

The main feature of the present investigation is a description of the full history of the gas stripping of the spiral galaxy outskirts and its consequent capture by a satellite during a parabolic encounter. Keeping in mind the recent observations of several interacting pairs of galaxies of comparable luminosities which demonstrate evidently ring-like structures in the making (see Introduction), we have considered a distant encounter of equal-mass systems. In the case of a distant encounter the effect of self-gravity may be ignored. The treatment of the gas hydrodynamics is described below.

We did not explore in a comprehensive manner the orbital parameter space and choose only one set of impact parameters for which the modelling encounter of an S0 galaxy with a gas-rich system of comparable mass unambiguously results in the polar-ring formation around the former. Motivated by the above observational data analysis, we have undertaken a numerical investigation of the ring-forming process for galaxies with different structures.

3.1.1. Method

Our simulations are based on a rather standard variant of the SPH code, which is the same as that in Sotnikova (1996). For simplicity, we adopt the smoothing length h (analogue of the particle size) to be independent of the local gas density. The smoothed values of hydrodynamical parameters are estimated by using a grid with cell length equal to $2h$. We assume an isothermal equation of state, leaving thermal effects completely unexplored. The gas is always at a temperature 10^4 K, and the corresponding equation of state is

$$P = c^2 \rho,$$

where P and ρ are the gas pressure and density, and $c = \text{const}$ is the isothermal speed of sound. For $T = 10^4$ K, $c \approx 9.1$ km/s.

The motion of $N = 10\,000$ particles, which represent elements of the continuous gaseous medium, is traced by means of equations of momentum conservation:

$$\frac{d\mathbf{r}_i}{dt} = \mathbf{v}_i, \quad (1)$$

$$\frac{d\mathbf{v}_i}{dt} = -\frac{1}{\rho(\mathbf{r}_i)}\nabla P(\mathbf{r}_i) + \mathbf{a}_i^{\text{visc}} - \nabla\Phi(\mathbf{r}_i), \quad (2)$$

where \mathbf{r}_i and \mathbf{v}_i are the spatial coordinate and velocity of the i -th particle, and Φ is the gravitational potential. The term $\mathbf{a}_i^{\text{visc}}$ describes the acceleration due to viscosity q_i :

$$\mathbf{a}_i^{\text{visc}} = -\frac{1}{\rho_i}\nabla q_i,$$

where $\rho_i = \rho(\mathbf{r}_i)$. We adopt one of the standard forms for the artificial viscosity q_i which serves to represent the sudden deceleration of the gas motion when strong shocks arise in the gas (e.g., Hernquist & Katz 1989):

$$q_i = \begin{cases} \alpha ch\rho_i|\nabla \cdot \mathbf{v}_i| + \beta h^2\rho_i|\nabla \cdot \mathbf{v}_i|^2, & \nabla \cdot \mathbf{v}_i \leq 0 \\ 0, & \text{otherwise.} \end{cases} \quad (3)$$

In the expression (3), the viscosity depends on the divergence of the velocity field. The first term is analogous to a bulk viscosity, the second, introduced to prevent particle interpenetration at high Mach number, is of the Neumann-Richtmyer type. Parameters α and β are free parameters. According to Hernquist & Katz (1989), one can satisfactorily reproduce the change of the density and pressure across the shock front if the values of α and β are equal to 0.5 and 1.0, respectively. We used just these numbers in our simulations.

The procedure of a smoothed-value estimation of the gas density is quite usual, as well as the transition from hydrodynamical equations (1) and (2) to SPH-equations (for a detailed description of the adopted numerical scheme, see Sotnikova 1996).

3.1.2. Model

Donor galaxy

To minimize the number of free parameters, we chose a very simple model for the donor galaxy – its potential was taken as that of a softened point mass

$$\Phi_0(r) = -\frac{GM_0}{(r^2 + a_0^2)^{1/2}}, \quad (4)$$

where G is the gravitational constant, M_0 the mass, and a_0 the softening scale length of the potential.

$N = 10\,000$ particles are used to represent the gaseous medium. They are initially gathered in a thin disk with a $1/r$ distribution from the center of the donor galaxy up to an outward radius R_0 and are placed in dynamically-cold circular orbits. The total gas mass is $0.2 M_0$. The gaseous particle size h , which determines the numerical spatial resolution, is 300 pc.

Throughout, we employ the following system of units: the gravitational constant $G = 1$, the mass of the donor galaxy $M_0 = 1$, the outer radius of the initial gas distribution in the donor galaxy $R_0 = 1$. In terms of physical units, a unit mass can be defined as $10^{11}M_\odot$, and a unit

distance corresponds to 15 kpc. Combined together, they give a unit time to be 86.6 Myrs, and a unit velocity to 169.3 km s^{-1} .

Accreting galaxy

We have considered the two-component model of a galaxy, consisting of a bulge and a disk. The light distribution of the bulge is well-provided by the model used, for example, in Weil & Hernquist (1993). For this model, the potential is

$$\Phi_b(r) = -\frac{GM_b}{r + a_b}, \quad (5)$$

where M_b is the bulge mass, and a_b the scale length of the potential.

The gravitational potential of the disk component of the galaxy is approximated by a Miyamoto & Nagai (1975) potential

$$\Phi_d(x, y, z) = -\frac{GM_d}{\sqrt{y^2 + z^2 + \left(b_d + \sqrt{x^2 + a_d^2}\right)^2}}, \quad (6)$$

where M_d is the disk mass, and a_d and b_d are scale radii. This model was favored by the simplicity of its practical usage. In our simulations, $a_d/b_d = 0.2$.

The ratio M_b/M_d determines the range of models from bulge-dominated systems (large values of the ratio) to disk-dominated galaxies (small values of the ratio). Four models for an accreting galaxy have been considered, with values of M_b/M_d equal to: 2.0, 1.0, 0.5, 0.2. The total mass of the galaxy is taken the same for all models and equal to that of the donor galaxy: $M_b + M_d = 1 = 10^{11}M_\odot$.

As shown in Section 2, main galaxies of PRGs with extended rings are similar to spiral galaxies in global photometric structure (and probably mass distribution). According to de Jong (1996), the bulge effective surface brightness shows the best correlation with morphological type of spiral galaxies. Therefore, the total bulge luminosity (mass) also correlates well. Scaling radii show a large scatter for all types of spiral galaxies. Thus, we fixed the scale lengths of galaxy components, leaving only the mass of the bulge to be variable. Scale lengths of the bulge a_b and disk b_d potentials are 1 kpc and 5 kpc, respectively. For these values, the half-mass radius of the bulge is $(1 + \sqrt{2})a_b \simeq 2.4$ kpc, and the maximum of the rotation curve of the disk component falls on the radius $\sqrt{2}(b_d + a_d) \simeq 8.4$ kpc.

Orbit

Before modelling a ring-forming encounter, we first solved the two-body problem for the donor and ring-host galaxies. The numerical procedure employed is quite similar to that used in Weil & Hernquist (1993).

Two interacting galaxies are initially separated by a rather large distance ($r_{\text{ini}} = 5 = 75$ kpc), so that tidal

effects be negligible. The initial velocities are taken as for parabolic encounter. The primary galaxy passes in a zero-inclination (in the plane of the gaseous disk of the donor galaxy – xy plane), prograde orbit (that is, the orbital angular momentum is parallel to the spin of the donor galaxy) with a pericenter distance r_{per} initially set as 1.6. The polar axis of the ring-host galaxy disk component (parallel to the x -axis) lies in the orbital plane, so the orbit is polar regarding the ring-host galaxy. The calculated orbit somewhat differs from parabolic (due to non-Keplerian potentials of galaxies), but its form is nearly the same for all models of a ring-host galaxy.

3.1.3. Results

During the encounter, the primary galaxy strips the outskirts of the donor object and a ring, rotating in the direction of the orbital motion, eventually forms around the galaxy in the encounter plane. As the equatorial plane of the disk component of S0 is taken to be perpendicular to that of the orbital motion, the ring is polar. The total amount of accreted gas is about 10% of all gas in the donor galaxy (or about $2 \times 10^9 M_{\odot}$) and there is not any significant difference in the stripped mass for all considered models of the ring-host galaxy. Some amount of the gas fell into the central part of galaxy. The mass of this gas is estimated as $2 \times 10^8 M_{\odot}$ within 1 kpc from the center. The timescale of the ring formation is a few 10^8 years. This time is somewhat shorter for rings forming around bulge-dominated galaxies and reaches up to $\sim 9 \times 10^8$ years for a disk-dominated model. The interacting galaxies are separated by a sufficiently large distance (more than 120 kpc) by the time of the ring steady-state settling, so that there are no any direct evidences of interaction between the galaxies and the ring-host system as an isolated object.

The simulations have revealed an interesting feature which appears during the ring-forming process in different galaxian potentials. As a steady state sets in, ring sizes begin to diverge. The results for four runs are presented in Figure 2.

Figure 2 gives a final stage of polar-ring formation for all considered models. This is the orbital plane projection of the gaseous rings. The marked difference in the ring structure is the difference in ring size, which rises when the bulge mass decreases and ranges from about 7 kpc in diameter for bulge-dominated systems (see Table 1) to approximately 13 kpc for disk-dominated objects.

The ring radius is finally determined by the angular momentum of donor galaxy gaseous particles forming the ring with respect to the galaxy at the moment of the pericenter passage. As the impact parameters are nearly the same for all runs, the value of the total angular momentum of ring-forming particles is almost the same for all models. But one can see from Figure 3 that the positions of particles with the same angular momentum are different for galaxies with different structures. Particles are closer to

the center of galaxy if there is a more concentrated mass distribution – the bulge-dominated model. This implies, in particular, that under the same conditions rings forming around elliptical galaxies with a strong concentration of mass to the center (see, for instance, the curves marked as $(* - * - *)$ and $(\circ - \circ - \circ)$ in Figure 3) should be less extended (on the average) – rather internal – than those around galaxies with a more gently sloping density profile (this fact was first mentioned in Sotnikova 1996).



Fig. 3. The angular momentum of a test particle on a circular orbit versus the distance from the center of a galaxy in the equatorial plane of the disk for 4 bulge-disk models. The short, medium and long dash lines conform to $M_b/M_d = 2.0, 1.0,$ and $0.5,$ correspondingly; the solid line gives $v_{\text{rot}}r - r$ relation for $M_b/M_d = 0.2.$ Two additional lines are shown as the bench-marks: $(* - * - *)$ – for diskless model, and $(\circ - \circ - \circ)$ – diskless model with more concentrated bulge ($a_b = 0.5$ kpc). The horizontal line marks the value of the mean angular momentum per ring particle for 4 runs.

In Figure 4, the surface density profiles along the major axes of the rings are shown. One can see one more interesting feature of simulated rings: rings farther from the center of the galaxy are more extended.

These results give the post factum justification of our impact parameter choice. Indeed, a closer passage results in less extended rings. The angular momentum of a gaseous particle at the moment of the closest approach of galaxies with respect the ring-host system is significantly affected by the term proportional to $\sim v_{\text{per}}r_{\text{per}},$ where v_{per} is the ring-host galaxy velocity relative to the donor galaxy. For parabolic encounters, it leads to $\sim \sqrt{r_{\text{per}}}.$ As the ring size monotonically decreases, the angular momentum decreases; a closer encounter gives a ring lying rather inside the galaxy. It is known that S0 galaxies possess some original gas, so the interaction between two gaseous systems would result in ring destruction. The further decreasing of pericenter distance leads to merging of the galaxies and total change of their structures. As to the more distant encounters, they do not allow capture of substantial amounts of gas, due to the sharp decrease of disturbing forces. We have repeated our runs with $r_{\text{per}} = 2.4 = 36$ kpc and have obtained that the mass of the resulting very diluted rings did not exceed $2 \times 10^8 M_{\odot}.$ Hyperbolic galaxy encounters are not efficient for ring formation, as the time of strong galaxy interaction is short. Let us note also that we discuss the properties of classic PRGs with optical star-forming rings. So we discuss the origin of relatively dense rings - with gas density large enough for star formation. This gives an additional restriction on the impact parameter, since the matter captured during the

Fig. 2. Time 10 (after the pericenter passage moment) frame for 4 runs. The values of the bulge to disk mass ratio of the ring-host galaxy are shown in the upper right-hand corner of all frames. All frames display the orbital plane (xy -plane) spatial projection and measure 30 kpc per edge. The equatorial plane of the ring-host galaxy disk component (parallel to yz -plane) is perpendicular to that of the orbital motion.

Fig. 4. Surface density profiles of rings. The short, medium and long dash lines conform to $M_b/M_d = 2.0, 1.0,$ and $0.5,$ correspondingly; the solid line - $M_b/M_d = 0.2.$

distant encounter will spread along a more extended orbit and will have lower mean density. Thus, galaxy encounters favourable to extended optical ring formation are extremely rare events. Such interactions must be between galaxies of specific types and within restricted geometry (polar encounters and a very narrow range of impact parameter).

We found in our simulations that, with the *same* impact parameter, the rings forming around bulge-dominated galaxies are less extended (by factor two) than the rings forming around disk-dominated galaxies. Therefore, having the same accretion history in the samples of elliptical and disk-type galaxies, we will have *on average* more extended rings around disk-dominated galaxies. This inference may explain in a quite natural manner the absence of extended polar rings around elliptical galaxies. It can also explain a difference in morphology of ionized gas in elliptical and S0 galaxies (Macchetto et al. 1996), assuming external origin of gas in these galaxies.

One can remark, however, that the obtained segregation of ring sizes (see Figure 2) is not as clear as the observed dichotomy (see Table 1). The simple bulge-disk model giving internal rings for bulge-dominated objects fails to explain the existence of very extended (up to 30 kpc in diameter) polar rings around disk-dominated galaxies. Probably, there exists one more physical factor leading to the strong differences of the PRG structural properties.

3.2. Exploration of dark halo inclusion effect

As it was found from the observational data analysis, there exists for PRGs with extended rings a remarkable structural resemblance of host galaxies to late-type spiral galaxies. It is known that dynamical properties of late-type spiral galaxies are determined to a considerable extent by invisible massive halos (e.g., Freeman 1992). Hence, we can suppose that PRGs with extended rings possess a third global component (besides the bulge and the disk) - a dark massive halo. The existence of dark massive halos also follows from the analysis of ring kinematics (e.g., Schweizer et al. 1983, Reshetnikov & Combes 1994a). To

account for the rotational velocities in the rings of UGC 7576 and UGC 9796 inside radii of 17 kpc and 21.4 kpc, respectively, one requires amounts of dark mass reaching 1.6 and 3 times the luminous masses (Reshetnikov & Combes 1994a).

What are the possible consequences of taking into account this structural component in the context of our investigation? As the gravitating mass of the primary galaxy increases, the orbital velocity of this galaxy relative to the donor object rises also. Then angular momentum arguments for a galaxy with such a structure lead to more distant orbits for captured particles.

We changed our bulge-disk model by adding a smoothed third component - a halo. The structure and the shape of dark halos in early-type galaxies appears to be, at present, an open question (Sackett et al. 1994, Combes & Arnaboldi 1996). For lack of unambiguous knowledge about the halo shape, we suppose the halo mass distribution to be spherical. As usual, halos are characterized by isothermal spheres over some radial interval. For simplicity, the following phenomenological cumulative mass profile is used to represent a halo in the present study:

$$M_h(r) = \frac{M_{h0}}{r_c} \left(r - a_h \arctan \left(\frac{r}{a_h} \right) \right) \left(1 - e^{-\frac{r_c}{r}} \right), \quad (7)$$

where M_{h0} is the total halo mass, r_c a cutoff radius, and a_h a core radius.

Our choice of halo parameters was determined by characteristic values obtained by Reshetnikov & Combes (1994a) from the ring kinematics investigation. The core radius a_h was taken as 9 kpc. The value of the cutoff radius r_{cut} is somewhat arbitrary and was taken to be equal to $3a_h$. We choose this value to give a reasonable halo mass outside the radius comparable with r_{per} . We have let the dark mass to be equal to twice the luminous mass (bulge + disk) inside a radius of 15 kpc. The total mass of the bulge and disk have been reduced, that is, $M_b + M_d = 0.5 = 5 \times 10^{10} M_\odot$, and we let $M_b/M_d = 0.01$, $a_b = 0.5$ kpc, $b_d = 3$ kpc.

The geometry of the encounter was the same as in previous numerical experiments. Expecting the capture of

gaseous matter on distant orbits and formation of a more diluted object, we have increased the total number of particles (up to 20 000) as well as their size h up to 375 pc to keep the gas treatment as a continuous medium.

The morphology of the new run is shown in Figure 5. By the time of $t = 6$ after the pericenter passage, the captured gaseous matter is azimuthally smeared in an annular configuration around the galaxy. This structure gradually evolves into a closed ring. We have followed its evolution up to $t = 20$. By this time, the ring was completely closed but not quite symmetric. According to Rix & Katz (1991) for a ring forming as a result of the gaseous satellite disruption, the smearing process takes up to seven orbital periods - up to 3-4 Gyrs or two times the final time of our run. The total mass gathered in the ring-like structure does not significantly differ from that obtained in haloless runs. The ring has a total mass of about $2.2 \times 10^9 M_\odot$. To explore the sensitivity of this value to the structural properties of the donor galaxy, we have constructed an additional model in which the spiral galaxy has its own halo. The parameters of this halo were taken the same as for the host galaxy. The mass of the captured gas turned out to be slightly smaller - $1.4 \times 10^9 M_\odot$. (This value is somewhat small in comparison with that obtained from observations. We omit the discussion of this question, because this value is obtained for one set of orbital parameters and we did not investigate the role of initial conditions, impact parameter, and structure of the donor galaxy. It may be impossible to understand the formation of very massive rings in the frame of the pure accretion scenario and the merging event is needed.)

The most remarkable feature of this annular structure is its size. The ring material lies well outside the luminous material of the host galaxy. We estimated the diameter of the ring of about 30 kpc. This value is typical of the objects of the first group of PRGs (see Table 1). The annular configuration obtained is rather narrow. Its further long-lived evolution will lead not only to azimuthal smearing of the gas but also to flattening of the radial density profile, forming a disk-like structure. Two factors promote the formation of rings with extended density distributions - the viscosity (see Rix & Katz 1991) and the nonsphericity of the potential (see Fig.5 in this paper and Fig.1 in Katz & Rix 1992).

4. Discussion and conclusions

We have analyzed the data on global structural properties of all known PRGs, and came to a conclusion that there is a correlation between the main characteristics of polar rings and host galaxies. There exist two different classes of PRGs: bulge-dominated galaxies with internal (relative to the optical size of a galaxy) rings and disk-dominated systems with extended rings. The sample studied is somewhat small (8-9 objects), but when we combine our prelim-

inary inference with the results of numerical experiments, a plausible picture of PRG properties emerges.

We have presented the investigation of the ring-forming process by studying the stripping of gas-rich galaxy outskirts during the encounter with galaxies of different structures and the subsequent settling of the captured material in the potential of a companion galaxy using an SPH method. The simulations have demonstrated that the ring sizes depend on galaxy potentials. *Under the same interaction conditions, rings twisting around galaxies with a strong concentration of mass to the center (bulge-dominated systems) are less extended (on the average) than that around disk-dominated galaxies.* Moreover, we have found that it is impossible to obtain very extended rings (with a diameter of about 30 kpc) taking into account the distribution of the luminous mass only. To obtain such extended rings, the galaxy mass distribution should be less concentrated than observed luminosity distribution. Therefore the presence of dark halos is required to explain the existence of extended rings.

One can suppose that the observational dichotomy is the result of selection. Indeed, interactions between galaxies accompanied by matter accretion occur with participation of various types of galaxies. But we have more chances to create long-lived extended rings when the accreting galaxy is a gas free, disk-like galaxy with extended massive dark halo. So such extended polar rings are expected to be observed preferably around specific types of galaxies.

The existence of the observational dichotomy suggests that PRGs with bulge-dominated central galaxies may possess less pronounced dark haloes in comparison with the first group of objects (another possibility - bulge-dominated galaxies have more centrally-concentrated halos - does not change our results as follow from Sect.3.1.3). These conclusions do not contradict the present-day observational data about dark halos in early-type galaxies (e.g., Bertin & Stiavelli 1993, de Zeew 1995). Nevertheless, we do not exclude other explanations of the revealed observational dichotomy (for instance, environmental influence etc.).

As was mentioned in Section 2, there is a close similarity between extended rings and disks of late-type spiral galaxies. Extended rings have the same total luminosities, integral colors, ratios of HI mass to the blue luminosity corrected for internal absorption, gas-to-dust ratios as normal spiral galaxies; there is evidence for the gaseous medium in polar rings to be near (or above) the gravitational stability limit, as the gaseous disks in spiral galaxies (Reshetnikov et al. 1994). Two polar rings (in UGC 7576 and UGC 9796) demonstrate H α -derived global star formation rates to be typical for normal spiral galaxies; general properties of HII regions in these galaxies are normal for late-type spirals (Reshetnikov & Combes 1994a). HII regions in the ring of prototype polar-ring galaxy NGC 2685 demonstrate nearly solar oxygen abundances

Fig. 5. Ring formation history for a galaxy with a massive halo. Dimensionless time (counted out from the moment of the minimum approach of galaxies) is given in the upper right-hand corner of all frames. The center of each frame coincides with the center of the ring-host galaxy. All frames show the orbital plane projection of the ring. The edge length of the frame corresponds to 80 kpc.

(Eskridge & Pogge 1994). Extended rings show radial color gradients with bluer colors at larger radii (Reshetnikov et al. 1994, Arnaboldi et al. 1995). The HI/H₂ mass ratio in the rings of NGC 660 and NGC 4650A is usual for spiral galaxies (Combes et al. 1992, Watson et al. 1994). There is evidence for the spiral structure in the rings of UGC 7576 (Reshetnikov & Combes 1994b) and NGC 4650A (Arnaboldi et al. 1996). There is an indication of the presence of a large-scale magnetic field in the ring of NGC 660 (Reshetnikov & Yakovleva 1991). Moreover, according to Combes & Arnaboldi (1996) and Arnaboldi et al. (1996), dark matter in PRGs could co-exist with the HI component, leaving its mark on the kinematics of the polar ring itself similar to the situation with a late-type galaxy gaseous disk. One can note finally that PRGs lie close to the Tully-Fisher relation for spiral galaxies (Knapp et al. 1985). Therefore, PRGs with extended rings could be undistinguishable from normal spiral galaxies at less advantageous orientation (with a more face-on ring) - see the discussion of this question in PRC. Probably, they will look like early-type spiral galaxies (maybe barred) with extended low surface brightness disks.

The striking similarity between extended rings and spiral disks suggests that PRGs are giant low surface-brightness spiral galaxies with decoupled bulges. Although this cannot be completely ruled out in some special cases, we suppose that the ring capture due to external accretion is a more frequent process (see Section 1 about observations of forming rings). Therefore, in contrast to the usual opinion that galactic interactions lead to fast morphological changes towards S0/E, the observational data on PRGs and our modelling simulations provide the example of a rare opposite shift - from an early-type gas-free galaxy through the capture of a gaseous disk to a spiral galaxy. One can suppose that PRG formation due to external accretion can imitate in some aspects the formation of disk galaxies in the hierarchically clustering model of the Universe (e.g., Steinmetz 1996).

In conclusion, let us reply shortly to the main questions of the article (see Section 1):

the accretion of matter from a gas-rich companion is a quite effective mechanism for polar-ring formation;

the spatial size of the forming ring is determined (under the same interaction conditions) by the mass distribution of the galaxy;

the process of ring formation takes approximately $(7-9) \times 10^8$ years for haloless systems and reaches up to a few Gyrs for host-galaxies possessing massive halos;

the total mass captured into the ring during an encounter with a gas-rich spiral galaxy exceeds $10^9 M_{\odot}$.

Acknowledgements. We would like to thank Françoise Combes and the referee (Linda Sparke) for helpful comments and criticism. VR acknowledges support from French Ministère de la Recherche et de la Technologie during his stay in Paris. This work was supported by grant N 94-02-06026-a from Russian Foundation for Basic Research.

References

- Arnaboldi M., Capaccioli M., Cappellaro E., Held E.V., Sparke L. 1993, A&A 267, 21
- Arnaboldi M., Freeman K.C., Sackett P.D., Sparke L.S., Capaccioli M. 1995, Planet. Space Sci. 43, 1377
- Arnaboldi M., Oosterloo T., Combes F., Freeman K.C., Koribalski B. 1996, AJ, submitted
- Bertin G., Stiavelli M. 1993, Rep. Prog. Phys. 56, 493
- Christodoulou D.M., Katz N., Rix H.-W., Habe A. 1992, ApJ 395, 113
- Combes F. 1994, in "The Formation and Evolution of Galaxies", C.Munoz-Tunon, F.Sanchez eds., Cambridge University Press, 376
- Combes F., Braine J., Casoli F., Gerin M., van Driel W. 1992, A&A 259, L65
- Combes F., Arnaboldi M. 1996, A&A 305, 763
- Cox A.L., Sparke L.S., Richter O., Shaw M. 1995, in "Proc. of the Ninth Annual Conference on Nonlinear Astronomy", in press
- Cox A.L., Sparke L.S. 1996, in "The Minnesota Lecture Series on Extragalactic Neutral Hydrogen", E.D.Skillman ed., PASP Conference Series, in press
- Curir A., Diaferio A. 1994, A&A 285, 389
- de Jong R.S. 1996, A&A 313, 45
- de Zeew P.T. 1995, in "Stellar Populations", P.C. van der Kruit, G.Gilmore eds., 215
- Eskridge P.B., Pogge R.W. 1994, BAAS 184, 4804
- Freeman K. 1992, in "Physics of Nearby Galaxies: Nature or Nurture?", T.X.Thuan, C.Balkowski, J.T.T.Van eds., Editions Frontieres, 201.
- Gingold R.A., Monaghan J.J. 1977, MNRAS 181, 375
- Hagen-Thorn V.A., Reshetnikov V.P. 1997, A&A 319, 430
- Hernquist L., Katz N. 1989, ApJS 70, 419
- Hibbard J.E., Mihos J.C. 1995, AJ 110, 140
- Katz N., Rix H.-W. 1992, ApJ 389, L55
- Keel W.C. 1996, Astrophys. Lett. & Commun., in press
- Knapp G.R., van Driel W., van Woerden H. 1985, A&A 142, 1

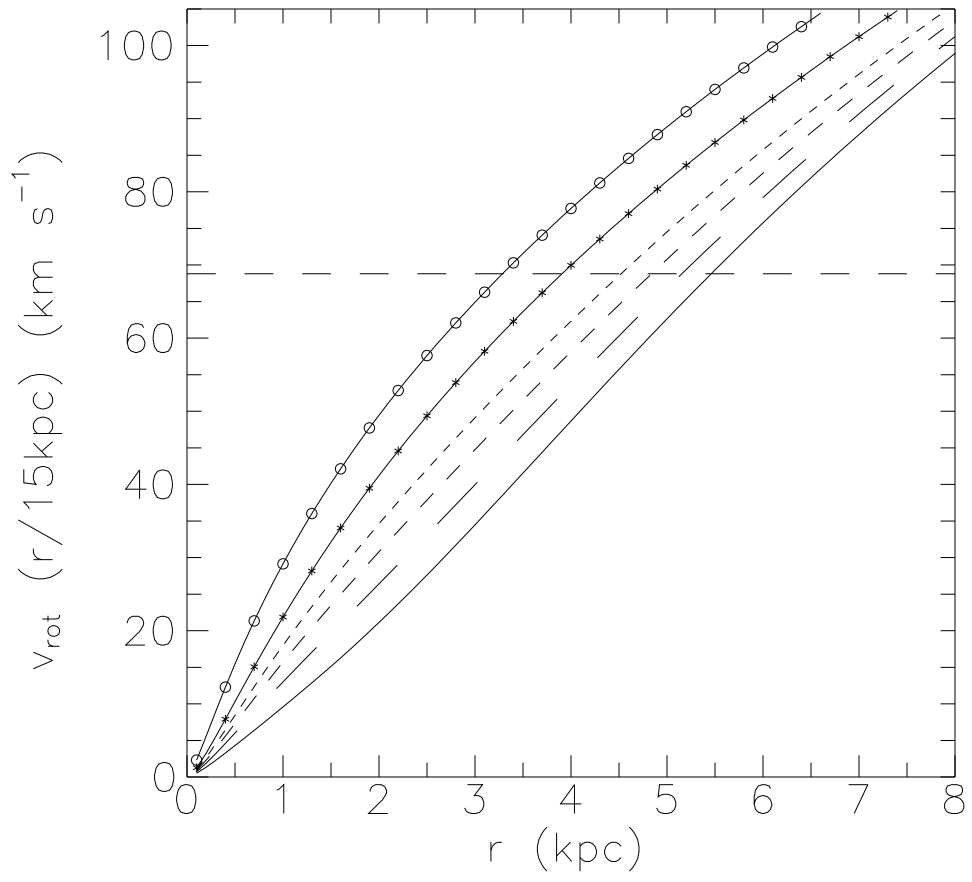
- Li J.G., Seaquist E.R. 1994, AJ 107, 1953
- Lucy L. 1977, AJ 82, 1013
- Macchetto F., Pastoriza M., Caon N. et al. 1996, A&AS 120, 463
- Makarov V.V., Reshetnikov V.P., Yakovleva V.A. 1989, Afz 30, 15
- Miyamoto M., Nagai R. 1975, PASJ 27, 533
- Reshetnikov V.P., Combes F. 1994a, A&A 291, 57
- Reshetnikov V., Combes F. 1994b, in “Violent Star Formation From 30 Doradus to QSOs”, G.Tenorio-Tagle ed., Cambridge University Press, 258
- Reshetnikov V.P., Hagen-Thorn V.A., Yakovleva V.A. 1994, A&A 290, 693
- Reshetnikov V.P., Hagen-Thorn V.A., Yakovleva V.A. 1995, A&A 303, 398
- Reshetnikov V.P., Hagen-Thorn V.A., Yakovleva V.A. 1996, A&A 314, 729
- Reshetnikov V.P., Yakovleva V.A. 1991, Afz 35, 61
- Richter O.-G., Sackett P.D., Sparke L.S. 1994, AJ 107, 99
- Rix H.-W., Katz N. 1991, in “Warped Disks and Inclined Rings around Galaxies”, S.Casertano, P.D.Sackett, F.H.Briggs eds., Cambridge University Press, 112
- Sackett P.D. 1991, in “Warped Disks and Inclined Rings around Galaxies”, S.Casertano, P.D.Sackett, F.H.Briggs eds., Cambridge University Press, 73
- Sackett P.D., Rix H.-W., Jarvis B.J., Freeman K. 1994, ApJ 436, 629
- Schechter P.L., Sancisi R., van Woerden H., Lynds C.R. 1984, MNRAS 208, 111
- Schweizer F., Whitmore B.C., Rubin V.C. 1983, AJ 88, 909
- Shane W.W. 1980, A&A 82, 314
- Sofue Y., Wakamatsu K. 1993, A&A 273, 79
- Sofue Y. 1994, ApJ 423, 207
- Sotnikova N.Ya. 1996, Afz 39, 259
- Sparke L.S. 1991, in “Warped Disks and Inclined Rings around Galaxies”, S.Casertano, P.D.Sackett, F.H.Briggs eds., Cambridge University Press, 85
- Steinmetz M. 1996, in “New Light on Galaxy Evolution”, R.Bender, R.Davies eds., Kluwer, in press
- Tohline J.E. 1990, in “Galactic Models”, J.R.Buchler, S.T.Gottesman, J.H.Hunter eds., New York, 198
- Toomre A. 1977, in “The Evolution of Galaxies and Stellar Populations”, B.M.Tinsley, R.B.Larson eds., Yale University Observatory, New Haven, 401
- van Gorkom J.H., Schechter P.L., Kristian J. 1987, ApJ 314, 457
- Watson D.M., Guptill M.T., Buchholz L.M. 1994, ApJ 420, L21
- Weil M.L., Hernquist L. 1993, ApJ 405, 142
- Whitmore B.C. 1991, in “Warped Disks and Inclined Rings around Galaxies”, S.Casertano, P.D.Sackett, F.H.Briggs eds., Cambridge University Press, 60
- Whitmore B.C., McElroy D.B., Schweizer F. 1987, ApJ 314, 439
- Whitmore B.C., Lucas R.A., McElroy D.B. et al. 1990, AJ 100, 1489 (PRC)

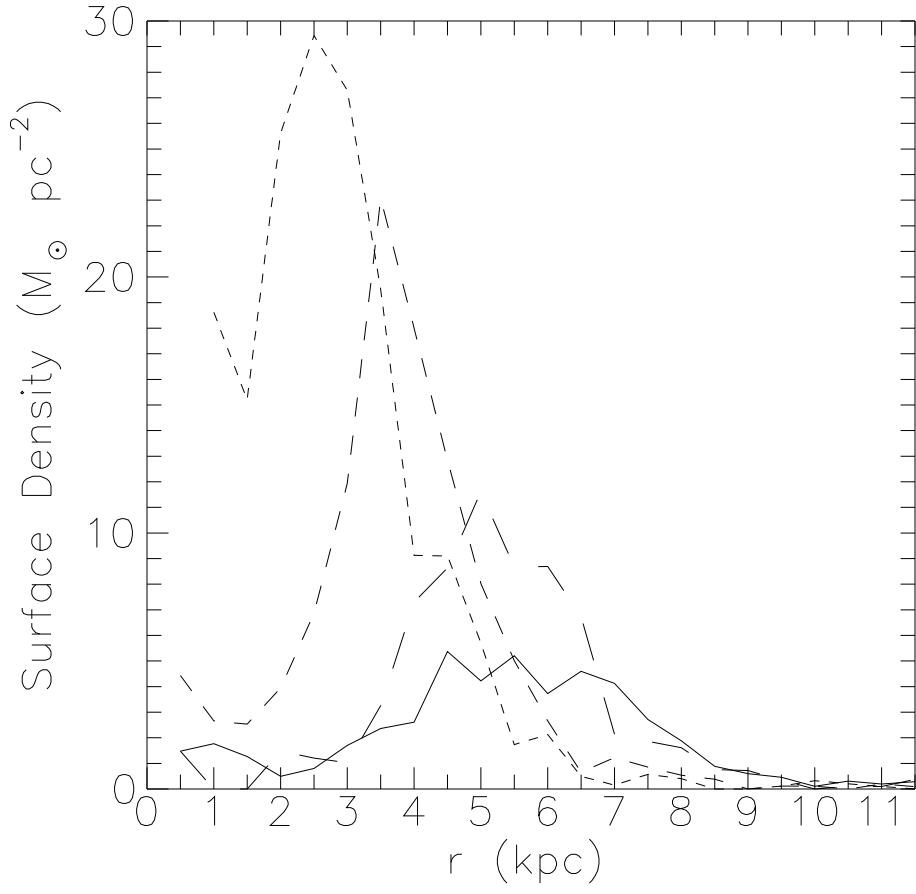
This figure "fig1.gif" is available in "gif" format from:

<http://arxiv.org/ps/astro-ph/9704047v1>

This figure "fig2.jpg" is available in "jpg" format from:

<http://arxiv.org/ps/astro-ph/9704047v1>





This figure "fig5.jpg" is available in "jpg" format from:

<http://arxiv.org/ps/astro-ph/9704047v1>